

# SEA ICE CHANGE DETECTION IN SAR IMAGES BASED ON COLLABORATIVE REPRESENTATION

Yunhao Gao<sup>1,2</sup>, Feng Gao<sup>1,2,\*</sup>, Junyu Dong<sup>1,2</sup>, Shengke Wang<sup>1,2</sup>

<sup>1</sup>College of Information Science and Engineering, Ocean University of China

<sup>2</sup>Qingdao Key Laboratory of Mixed Reality and Virtual Ocean, Ocean University of China

## ABSTRACT

Sea ice change detection from synthetic aperture radar (SAR) images is important for navigation safety and natural resource extraction. This paper proposed a sea ice change detection method from SAR images based on collaborative representation. First, neighborhood-based ratio is used to generate a difference image (DI). Then, some reliable samples are selected from the DI by hierarchical fuzzy C-means (FCM) clustering. Finally, based upon these samples, collaborative representation method is utilized to classify pixels from the original SAR images into unchanged and changed class. From there, the final change map can be obtained. Experimental results on two real sea ice datasets demonstrate the superiority of the proposed method over two closely related methods.

**Index Terms**— synthetic aperture radar; sea ice change detection; clustering method; collaborative representation.

## 1. INTRODUCTION

The Arctic and Antarctic sea ice monitoring has been paid more and more attentions recently, since the change information of sea ice is important for navigation safety and natural resource extraction. Many techniques have been applied for sea ice change detection by using multimodal remote sensing data, such as optical, hyperspectral, and synthetic aperture radar (SAR) data.

Among the aforementioned multimodal data, SAR is the ideal source for sea ice change detection [7], since SAR sensors have the ability of acquiring images under all-time and all-weather conditions. Moreover, with the development of earth observation programs, more and more SAR sensors have been developed to collect images for the same geographical area at shorter intervals. However, sea ice change detection with SAR images exhibits difficulties due to the presence of multiplicative speckle noise. How to alleviate

the interference of multiplicative speckle noise has become a critical issue in SAR image applications.

The first step of change detection is difference image (DI) generation. Many techniques have been proposed to suppress the speckle noise in DI generation. Hou *et al.* [2] presented a fusion strategy to combine the Gauss-log ratio image and the log-ratio image together. The speckle noise can be reduced in the fused difference image. Gong *et al.* [6] proposed a neighborhood-based ratio (NR) operator to generate difference image for SAR change detection. The NR operator takes the spatial information into consideration, and therefore works better in suppressing speckle noise than the traditional log-ratio operator.

After DI generation, SAR change detection is usually treated as a classification task, and the pixels in the DI are classified into changed and unchanged class by using expectation maximization (EM) algorithm [4], fuzzy c-means clustering (FCM) [5], support vector machines [7], etc. Gao *et al.* [5] presented a hierarchical FCM clustering algorithm for SAR change detection. The FCM algorithm is implemented in a coarse-to-fine procedure, and the change detection performance is greatly improved. Wang *et al.* [7] presented a SAR image change detection method based on Laplacian SVM. Some labeled samples are selected from the DI. Laplacian SVM explores the change information from these samples, and the discriminative power in changed pixels identification is enhanced.

Recently, collaborative representation [8] has drawn the attentions of researchers in remote sensing application community. Li and Du [9] developed a collaborative representation-based method with spatial and spectral features for hyperspectral image classification. Jiang *et al.* [10] proposed a hyperspectral image classification method incorporating the spatial information by adding a spatial regularization term to the representation objection function of collaborative representation. Inspired by these works, collaborative representation can exploit the spatial information of neighborhood pixels in classification. Therefore, it may suppress the multiplicative speckle noise by utilizing spatial information, and the change detection performance can be improved.

In this paper, a novel sea ice change detection method

This work was partially supported by the National Natural Science Foundation of China under Grant 41606198 and 41576011, and Natural Science Foundation of Shandong Province under Grant ZR2016FB02. (Email: gaofeng@ouc.edu.cn)

in SAR images based on collaborative representation is proposed. First of all, neighborhood-based ratio is utilized for DI generation. Secondly, hierarchical FCM algorithm is employed to select reliable samples. Finally, based upon these samples, collaborative representation method is utilized to classified pixels from the original SAR images into unchanged and changed class. From there, the final change map can be obtained. Experimental results on two real sea ice datasets demonstrate the superiority of the proposed method over two closely related methods.

## 2. METHODOLOGY

Two multitemporal sea ice images  $I_1$  and  $I_2$  acquired by SAR sensors at the same polar region are considered as the input images. The main objective of change detection is to generate a change map which gives the interpretations about the changes occurred. Change identified between two images can be modeled as a binary classification problem. The framework of the proposed method is illustrated in Fig. 1.

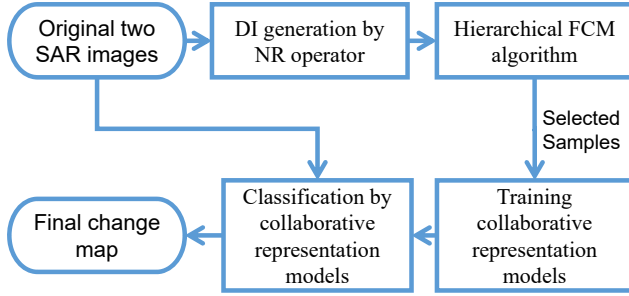


**Fig. 1.** Framework of the proposed change detection method

The proposed method is composed of three steps: 1) DI generation by neighborhood-based ratio operator; 2) Reliable sample selection by hierarchical FCM algorithm; 3) Model training and classification by collaborative representation. The detailed descriptions of Step 1 and Step 2 are given in Section 2.1. The descriptions of Step 3 are provided in Section 2.2.

### 2.1. DI Generation and Reliable Sample Selection

In order to obtain reliable training samples pixels, we employ similar strategies as mentioned in [5]. First, NR operator [6] is utilized to generate a DI. The operator is defined as:

$$DI(p) = (1 - \theta) \times \frac{\sum_{i \in \Omega \wedge i \neq p} \min\{I_1(p), I_2(p)\}}{\sum_{i \in \Omega \wedge i \neq p} \max\{I_1(p), I_2(p)\}} + \theta \times \frac{\min\{I_1(p), I_2(p)\}}{\max\{I_1(p), I_2(p)\}}, \quad (1)$$

$$\theta = \frac{\sigma(p)}{\mu(p)}, \quad (2)$$

where  $DI(p)$  is the gray level of a pixel at position  $p$  in the DI. It indicates the local similarity between  $I_1$  and  $I_2$ .  $\sigma(p)$  and  $\mu(p)$  denote the variance and mean of the gray level in neighborhood, respectively. The size of neighborhood region is  $r \times r$  pixels. The coefficient  $\theta$  is a measure of the local heterogeneity: When the local area is homogeneous,  $\theta$  often reaches low value; When the local area is heterogenous,  $\theta$  often reaches high value.

After obtaining the DI, hierarchical FCM algorithms is employed. The detailed descriptions of the algorithm can be found in [5]. After classification, some reliable samples of high probability to be changed or unchanged are selected as training samples for collaborative representation.

### 2.2. Collaborative Representation

In image classification studies, a common idea is to represent a test sample by the training samples and assign the test sample a label which provides the lowest reconstruction residual. Sparse representation method is such a strategy, and has been applied in various image classification applications [11]. However, Zhang *et al.* [8] argued that collaborative representation is the determining factor rather than sparse representation that improves the classification performance.

It is widely acknowledged that the “collaborative” nature of the approximation improves the classification accuracy. Specifically, in pixelwise classification, one pixel is likely to be assigned the same label as its neighborhood pixels. Therefore, the contextual information is very important and needs to be taken into consideration. We first extract neighborhood features for each pixel. Let  $V_p^{I_1}$  represent a patch centered at position  $p$  in image  $I_1$ , and  $V_p^{I_2}$  represent a patch centered at position  $p$  in image  $I_2$ . The size of both patches is  $k \times k$ . Both image patches are converted to vectors and concatenated to form a new vector  $V_p$ . Therefore, the  $V_p$  is considered to contain enough changed information around the center pixel  $p$ . Supposing that there are  $N$  pixels in the original image,  $X = [x_1, x_2, \dots, x_m] \in \mathbb{R}^{2k^2 \times m}$  ( $m < N$ ) is the training set with classes. The optimal representation coefficient  $\alpha^*$  can be derived as:

$$\alpha^* = \arg \min_{\alpha} \{\|y - X\alpha\|_2^2 + \lambda \|\Gamma\alpha\|_2^2\}, \quad (3)$$

Here,  $y$  is the testing set.  $\lambda$  is the regularization coefficients, and  $\alpha$  is the representation coefficient. The minimization of regularization terms and residual would be balanced by the parameter  $\lambda$ .  $\Gamma$  is a biasing Tikhonov matrix defined by  $\Gamma = \|y - x_i\|_2, i = 1, 2, \dots, N$ . Therefore, the optimal representation coefficients can be redefined as:

$$\alpha^* = (X^T X + \lambda \Gamma) X^T y^T, \quad (4)$$

After obtaining the optimal representation coefficient  $\alpha^*$ , the label of the testing set can be calculated through minimizing the regularization terms and residual:

$$\text{class}(y) = \arg \min \|y - X_l \alpha_l^*\|_2^2, \quad (5)$$

where  $l = 1$  means the label of changed class, while  $l = 0$  means the label of unchanged class.

### 3. EXPERIMENTAL RESULTS AND ANALYSIS

#### 3.1. Experiment Setup

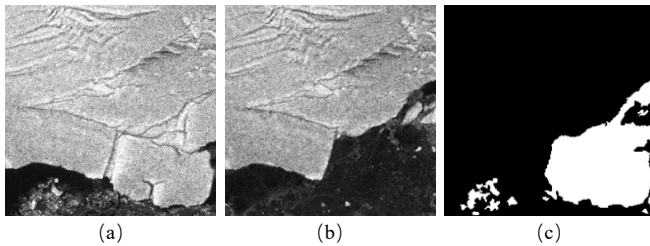


**Fig. 2.** Dataset I from Sulzberger Ice shelf. (a) Image acquired in March 11 in 2011. (b) Image acquired in March 16 in 2011. (c) Ground truth image.

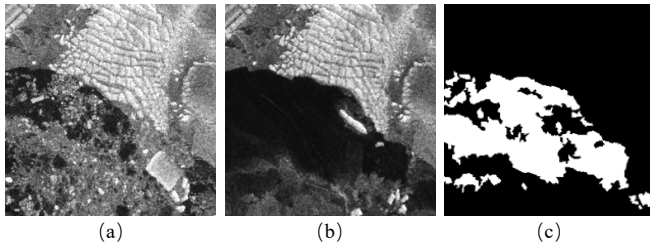


**Fig. 3.** Dataset II from Sulzberger Ice shelf. (a) Image acquired in March 11 in 2011. (b) Image acquired in March 16 in 2011. (c) Ground truth image.

In order to verify the effectiveness of the proposed method in sea ice change detection, we will show the performance of the proposed method on two real SAR datasets. Both datasets are selected from two large SAR images of the region of the Sulzberger Ice Shelf, and the images are captured by the European Space Agency’s Envisat satellite on March 11 and 16, 2011. Both images show the progression of the ice breakup. The ice breakup are triggered by Tohoku Tsunami in the Pacific Ocean on March 11 in 2011. The Tohoku Tsunami generated massive ocean waves. These waves caused the Sulzberger Ice Shelf to flex and break. The original size of both SAR images is  $2263 \times 2264$  pixels. They are too huge to show the detailed information. Therefore, we select two

typical areas ( $256 \times 256$  pixels for each area). Both datasets and the available ground truth images which are obtained are shown by integrating prior information with photo interpretation. Dataset I is shown in Fig. 2, and Dataset II is shown in Fig. 3.

The performance evaluation of change detection is a critical issue. We use false positives (FP), false negatives (FN), overall error (OE), percentage of correct classification (PCC) as indicators to measure the effectiveness of the proposed method. The FP is the number of pixels that are unchanged pixels in the ground truth image but wrongly classified as changed ones. The FN is the number of pixels that are changed class in the ground truth image but wrongly classified as unchanged ones. The OE is computed by  $OE = FP + FN$ . The PCC is computed by  $PCC = (1 - OE/Nt) \times 100\%$ , where  $Nt$  represents the total pixels in the ground truth image.

#### 3.2. Results on the Dataset I

In order to verify the effectiveness of the proposed sea ice change detection method, we compare our method with two closely related methods: PCAKM [12] and GaborPCANet [13]. The final change detection maps are shown in figure form and the criteria are shown in tabular form.

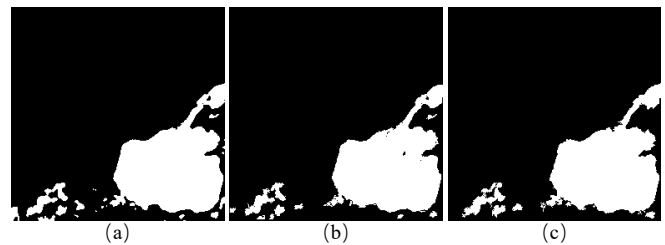


**Fig. 4.** Visualized results of change detection methods on Dataset I. (a) Result by PCAKM [12]. (b) Result by GaborPCANet [13]. (c) Result by the proposed method.

**Table 1.** Change detection results on Dataset I.

Methods	FP	FN	OE	PCC(%)
PCAKM [12]	711	479	1190	98.18
GaborPCANet [13]	422	724	1146	98.25
Proposed method	429	464	893	98.64

Fig. 4 shows the final change maps of different methods on Dataset I, and Table 1 lists the specific values for evaluation criteria. We can observe that there are some noisy white spots in the results generated by PCAKM. Therefore, the FP value of PCAKM is relatively high. As shown in Fig. 4(b), some important changed regions are missed by GaborPCANet, and the FN value of GaborPCANet is relatively high.

The OE and PCC values of the proposed method achieves better performance than the other methods. It proves that the proposed method can obtain satisfactory results and can effectively suppress the multiplicative speckle noise.

### 3.3. Results on the Dataset II

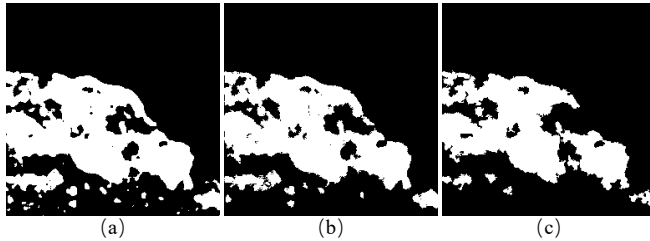


**Fig. 5.** Visualized results of change detection methods on Dataset II. (a) Result by PCAKM [12]. (b) Result by GaborPCANet [13]. (c) Result by the proposed method.

**Table 2.** Change detection results on Dataset II.

Methods	FP	FN	OE	PCC(%)
PCAKM [12]	3215	141	3356	94.88
GaborPCANet [13]	2237	599	2836	95.67
Proposed method	1181	1360	2541	96.12

Fig. 5 shows the change detection results on Dataset II. Evidently, the PCAKM and GaborPCANet are contaminated severely by the speckle noise, and there are many noisy white spot in the generated change maps. Therefore, the FP values of PCAKM and GaborPCANet are much higher than the proposed method. The proposed method produces fewer false alarms and it suppresses the bad effects of multiplicative speckle noise. The quantitative and qualitative comparison on the dataset has demonstrated the superiority of the proposed method.

## 4. CONCLUSION

This paper presented a novel sea ice change detection method for SAR images based on collaborative representation. First, neighborhood-based ratio is utilized for DI generation. Secondly, hierarchical FCM algorithm is employed to select reliable samples. Finally, collaborative representation method is utilized to classify pixels from the original SAR images into unchanged and changed class. Experimental results on two real sea ice datasets demonstrate the effectiveness of the proposed method. Compared with other closely related works, collaborative representation has presented good performance in sea ice change detection.

## 5. REFERENCES

- [1] L. Wang *et al.*, "Sea ice concentration estimation during melt from dual-pol SAR scenes using deep convolutional neural networks: A case study," *IEEE Trans. Geosci. Remote Sens.*, vol. 54, no. 8, pp. 4524–4533, 2016.
- [2] B. Hou *et al.*, "Unsupervised change detection in SAR image based on gauss-log ratio image fusion and compressed projection," *IEEE J. Sel. Top. Appl. Earth Obs. Remote Sens.*, vol. 7, no. 8, pp. 3297–3317, 2014.
- [3] M. Gong, Y. Cao, and Q. Wu, "A neighborhood-based ratio approach for change detection in SAR images," *IEEE Geosci. Remote Sens. Lett.*, vol. 9, no. 2, pp. 307–311, 2012.
- [4] L. Bruzzone and D. F. Prieto, "Automatic analysis of the difference image for unsupervised change detection," *IEEE Trans. Geosci. Remote Sens.*, vol. 38, no. 3, pp. 1171–1182, 2000.
- [5] F. Gao *et al.*, "Change detection from synthetic aperture radar images based on neighborhood-based ratio and extreme learning machine," *J. Appl. Remote Sens.*, vol. 10, no. 4, 2016.
- [6] M. Gong, Y. Cao, Q. Wu, "A neighborhood-based ratio approach for change detection in SAR images," *IEEE Geosci. Remote Sens. Lett.*, vol. 9, no. 2, pp. 307–311, 2012.
- [7] S. Wang, S. Yang, L. Jiao, "Saliency-guided change detection for SAR imagery using a semi-supervised Laplacian SVM," *Remote Sens. Lett.*, vol. 7, no. 11, pp. 1043–1052, 2016.
- [8] L. Zhang, M. Yang and X. Feng, "Sparse representation or collaborative representation: Which helps face recognition?" in *Proc. ICCV*, 2011, pp. 471–478.
- [9] W. Li and Q. Du, "Joint within-class collaborative representation with multitask learning for hyperspectral image classification," *IEEE Trans. Geosci. Remote Sens.*, vol. 52, no. 6, pp. 3707–3719, 2014.
- [10] J. Jiang *et al.*, "Spatial-aware collaborative representation for hyperspectral remote sensing image classification," *IEEE Geosci. Remote Sens. Lett.*, vol. 14, no. 3, pp. 404–408, 2017.
- [11] W. Song, P. Liu, and L. Wang, "Sparse representation-based correlation analysis of non-stationary spatiotemporal big data," *Int. J. Digit. Earth*, vol. 9, no. 9, pp. 892–913, 2016.
- [12] T. Celik, "Unsupervised change detection in satellite images using principal component analysis and k-means clustering," *IEEE Geosci. Remote Sens. Lett.*, vol. 6, no. 4, pp. 772–776, 2009.
- [13] F. Gao *et al.*, "Automatic change detection in synthetic aperture radar images based on PCANet," *IEEE Geosci. Remote Sens. Lett.*, vol. 13, no. 12, pp. 1792–1796, 2016.